Fuel cladding chemical interaction of irradiated U-Zr fuel with Fe based cladding materials at high temperatures

Ju-Seong Kim, June-Hyung Kim, Byoung-Oon Lee,
Yang-Hong Jung, Boung-Ok Yoo,Young-Jun Kim, and Jin-Sik Cheon
Korea Atomic Energy Research Institute, 989-111 Daedeokdaero, Yuseong-gu, Daejeon, 34057, Korea
*Corresponding author: juskim@kaeri.re.kr

1. Introduction

U-Zr based fuels and ferritic-martensitic stainless (FMS) steel claddings have been considered as the most probable fuel for the initial core of the sodium-cooled fast reactor (SFR) [1]. In this study, to investigate the FCCI reaction of metallic fuel under a transient condition, high-temperatures heating tests were performed with irradiated U-10Zr fuel slugs with T92 cladding at hot-cell in Korea Atomic Energy Research Institute (KAERI). After the heating test, the microstructures of fuel and cladding are observed through an optical microscope (OM), scanning electron microscope (SEM), and element distribution was analyzed by using electron probe micro analyzer (EPMA).

2. Experimental

2.1 Materials

The fuel rod of U-10wt%Zr with T92 (NF616) cladding was irradiated in the HANARO test reactor at KAERI [2]. The fuel rods were irradiated for 182 effective full power days (EFPDs). The LHGR of the fuel rod is between 120 W/cm and 245 W/cm, and the average burn-up of 2.9 at% can be achieved. Fig. 1 shows the X-ray image of the irradiated U-10Zr fuel rod. The fuel slug was cut into five segments using low speed saw for four specimens for FCCI tests and one specimen for observation of as-irradiated state of the specimen.

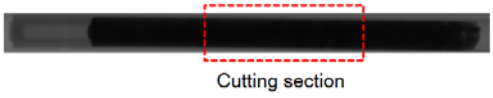

Fig. 1. Transmitted X-ray image of the irradiated U-10Zr fuel rod.

A special jig for a transient test was designed and manufactured to facilitate easy handling by manipulators in hot-cell. Fig. 2 shows a schematic diagram of the jig. As shown in the figure, the top and the bottom surfaces of the specimens can get into contacts with the FC92, and HT9 plates, which enables to induce an inter-diffusion reaction of the fuel slug with T92, FC, and HT9, simultaneously.

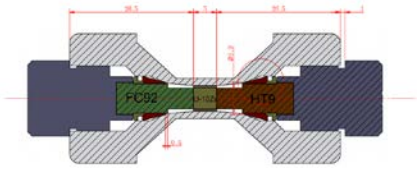

Fig. 2. Schematics of the jig for fuel cladding chemical interaction.

Fig. 3 Specimen assembling in Hot-cell

Fig. 3 shows the specimen handling image in Hot-cell. After the specimen assembling, mechanical contacts between fuel slug and clad materials were confirmed by X-ray image as shown in Fig. 4. To evaluate the penetration depth of cladding by a eutectic reaction, the transient tests were conducted at 800 °C for 1 hr. After the transient tests, the specimen in the jig was quenched in water, and then, the X-ray transmission of the holder was also performed to check the FCCI reaction of specimen indirectly. As shown in the figure, mechanical contacts were made before the test, and unknown reaction products were observed after the test which seems to be a liquid phase of U-Fe. To observe microstructure of the specimen, both sides of the dog bone type of the jig was cut and mounted. The microstructures of the fuel slug and clad material were observed using optical microscopy (OM) and SEM equipped with wavelength dispersive X-ray spectroscopy (WDS) in an electron probe micro analyzer (EMPA, JXA-8320 JEOL). Moreover, to compare before and after the reaction, metallography of the as-irradiated fuel slug was also observed.

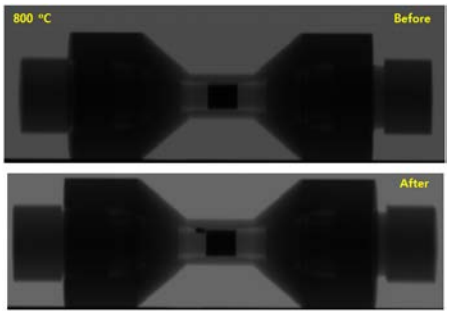

Fig. 4. X-ray images of the holder before and after the test

3. Results and discussion

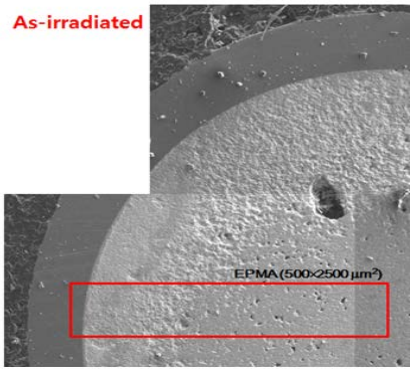

Fig. 5 SEM image of as-irradiated U-10Zr

Fig. 5 shows the transverse cross section of as-irradiated U-10Zr rod. X-ray mapping was conducted in radial direction in Fig. 5 with the major fuel and cladding elements U, Zr, Fe, Cr, and Nd. Fig. 6 shows quantitative X-ray map of the U, Zr, Fe, Cr, and Nd in radial direction and average intensity profile results of the X-mapping. The average intensity profile indirectly indicates the average value of the element concentration, which is essential in analyzing material characterization. As shown in the figure, the concentration of Zr is highest at the center and decreases with increase in distance from the center, whereas U concentration seemed to be a little complicated but U is deemed to follow the trends that U balances the total mass. It is noted that the maximum centerline temperature of this specimen was calculated to be 549 °C [3], which is far below the phase transition temperature of the U-Zr phase diagram [4], and therefore the fuel slug will be operated in the single $\alpha+\delta$ phase during HANARO irradiation, Thus, there will be no effects of chemical potential and it is concluded that the concentration profile of the Zr is good agreement with the temperature profile history of the fuel.

Fission yield of Nd and Ce is largest among the lanthanides. Lanthanides have been observed in pore and periphery of the fuel slug. It is known that lanthanide fission products tend to migrate the peripheral zone of fuel through the inter-connected pores. As shown in the figure, agglomerated Nd particle dispersed in the U-Zr matrix and also observed in the fuel cladding interface.

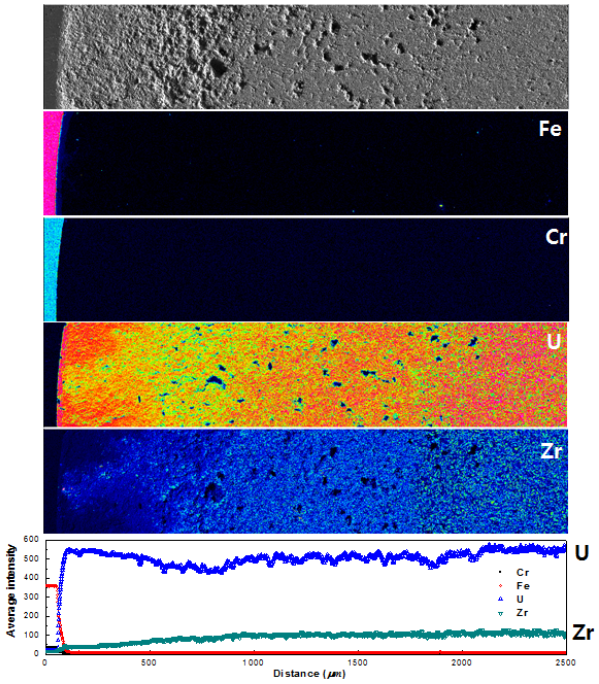

Fig. 6. X-mapping of the elements in the specimen and distribution along the radial direction.

Fig. 7 shows the cross-section on the radial-axial plane of the specimen. Yellow dash line in the figure is the initial fuel cladding boundary. As shown in the figure, a significant FCCI occurred uniformly along the cladding materials of T92, but FCCI between fuel and un-irradiated clad materials (HT9 and FC92) seems to not occur in the both clad materials.

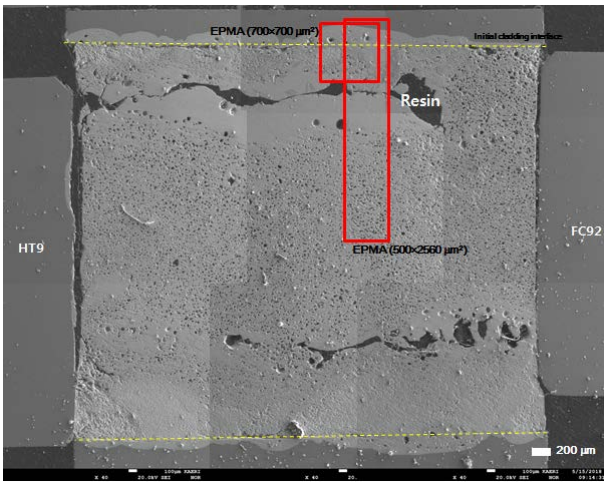

Fig. 7. SEM image of the specimen after the tests

It is thought that owing to misalignment of fuel and

cladding, and surface roughness of the fuel, the contacts of the fuel and clad materials are not perfect. As shown in the figure, the central area shows the typical irradiated microstructure of the metallic fuel heated high temperature but the microstructure near the FCCI region is different.

The quantitative X-ray mappings were conducted for the element distribution of the specimen in the radial direction. Fig. 9 shows the X-ray maps and the average X-ray count profile in the maps. As shown in the figure, the diffused length of Fe is much longer than that of U. During the 1 hr at 800 °C, Fe diffused 1200 μm toward U-Zr matrix while U migrates to 250 μm toward Fe-Cr matrix. The concentration profile of Cr seems to follow that of Fe. In Fig. 9, empty space was observed in the reaction region; however, which is identified as mounting resin as shown in Fig.7. It is thought that during the re-mounting the mounting resin would fill the empty hole. The Nd distribution in Fig. 8 shows that Nd is concentrated on the periphery of the resin, which corroborates that the area where empty space observed is deemed to have consisted of brittle materials such as lanthanides.

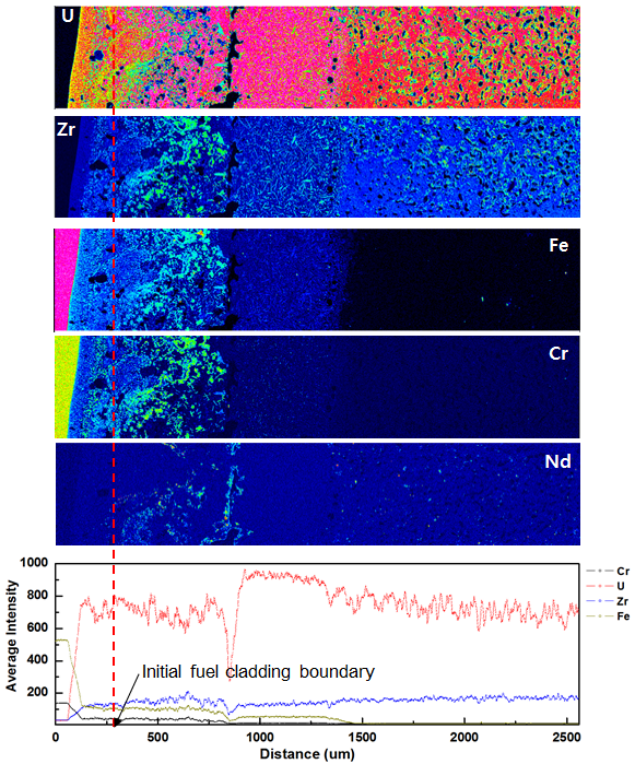

Fig. 8. X-mapping of the elements in the specimen and distribution along radial direction after being heated at 800 °C for 1hr

Fig. 9 shows the penetration rate of irradiated fuels during high temperature heating tests. As shown in the figure, the penetration of this study is slightly higher than the maximum cladding penetration rate of the previous studies [5]. Further tests will be conducted in the near future.

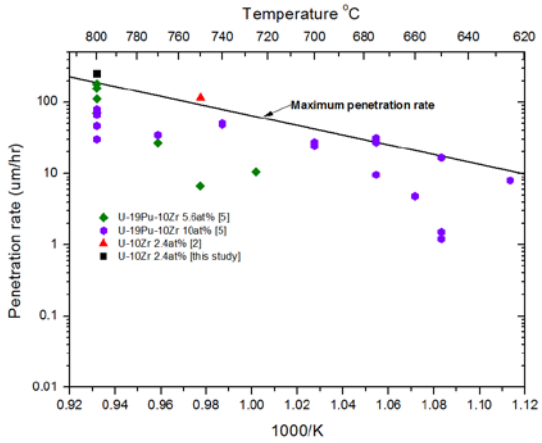

Fig. 9. Penetration rate as a function of test temperature

4. Summary and conclusions

High temperature heating test was conducted with irradiated U-10Zr and T92 cladding in Hot-cell. Following conclusions can be drawn.

- The concentration profile of the Zr in as-irradiated condition is good agreement with the temperature history of the fuel.
- During the 1 hr at 800 °C, Fe diffused 1200 μm toward U-Zr matrix while U migrates to 250 μm toward Fe-Cr matrix.

ACKNOWLEDGEMENT

This project has been carried out under the Nuclear R&D program by Ministry of Science, ICT & Future Planning.

REFERENCES

[1] C.B. Lee, J.S. Cheon, S.H. Kim, J.-Y. Park, H.-K. Joo, Nuclear Engineering and Technology 48 (2016) 1096-1108.
[2] J.-H. Kim, J.-S. Cheon, B.-O. Lee, J.-H. Kim, H.-M. Kim, B.-O. Yoo, Y.-H. Jung, S.-B. Ahn, C.-B. Lee, Metals and Materials International 23 (2017) 504-511.
[3] B.O. Lee, J.S. Cheon, C.B. Lee, Performance limit analysis of a metallic fuel for Kalimer, American Nuclear Society - ANS, La Grange Park (United States); American Nuclear Society, 555 North Kensington Avenue, La Grange Park, IL 60526 (United States), 2007, p. Medium: X; Size: page(s) 397-403.
[4] R.I. Sheldon, D.E. Peterson, Bulletin of Alloy Phase Diagrams 10 (1989) 165-171.
[5] A.B. Cohen, H. Tsai, L.A. Neimark, Journal of Nuclear Materials 204 (1993) 244-251.